AGU PUBLICATIONS

JGR

Journal of Geophysical Research: Biogeosciences

RESEARCH ARTICLE

10.1002/2014JG002780

Key Points:
- Overestimated LAI in both models caused a positive net radiation bias
- LE biased low from July to September in both models due to underestimated SWC
- The two crop models underestimated carbon emissions

Supporting Information:
- Supporting Information S1

Correspondence to:
M. Chen,
chen1718@umn.edu

Citation:
Chen, M., T. J. Griffis, J. Baker, J. D. Wood, and K. Xiao (2015), Simulating crop phenology in the Community Land Model and its impact on energy and carbon fluxes, *J. Geophys. Res. Biogeosci.*, *120*, 310–325, doi:10.1002/2014JG002780.

Received 21 AUG 2014
Accepted 24 JAN 2015
Accepted article online 28 JAN 2015
Published online 26 FEB 2015

Simulating crop phenology in the Community Land Model and its impact on energy and carbon fluxes

Ming Chen[1], Tim J. Griffis[1], John Baker[1,2], Jeffrey D. Wood[1], and Ke Xiao[1]

[1]Department of Soil, Water, and Climate, University of Minnesota-Twin Cities, Saint Paul, Minnesota, USA, [2]USDA-ARS, Saint Paul, Minnesota, USA

Abstract A reasonable representation of crop phenology and biophysical processes in land surface models is necessary to accurately simulate energy, water, and carbon budgets at the field, regional, and global scales. However, the evaluation of crop models that can be coupled to Earth system models is relatively rare. Here we evaluated two such models (CLM4-Crop and CLM3.5-CornSoy), both implemented within the Community Land Model (CLM) framework, at two AmeriFlux corn-soybean sites to assess their ability to simulate phenology, energy, and carbon fluxes. Our results indicated that the accuracy of net ecosystem exchange and gross primary production simulations was intimately connected to the phenology simulations. The CLM4-Crop model consistently overestimated early growing season leaf area index, causing an overestimation of gross primary production, to such an extent that the model simulated a carbon sink instead of the measured carbon source for corn. The CLM3.5-CornSoy-simulated leaf area index (LAI), energy, and carbon fluxes showed stronger correlations with observations compared to CLM4-Crop. Net radiation was biased high in both models and was especially pronounced for soybeans. This was primarily caused by the positive LAI bias, which led to a positive net long-wave radiation bias. CLM4-Crop underestimated soil water content during midgrowing season in all soil layers at the two sites, which caused unrealistic water stress, especially for soybean. Future work regarding the mechanisms that drive early growing season phenology and soil water dynamics is needed to better represent crops including their net radiation balance, energy partitioning, and carbon cycle processes.

1. Introduction

The impact of climate change on future crop system production and food security remains an important global issue [*Karl et al.*, 2009; *Piao et al.*, 2010; *Lobell et al.*, 2011; *Ma et al.*, 2012; *Rosenzweig et al.*, 2013; *Yin*, 2013]. Predicting the impact of future climate change on agricultural systems requires incorporation of mechanistic crop biophysical processes and interactive crop management into climate models, which remains relatively rare [*Rosenzweig et al.*, 2013]. An accurate representation of dynamic crop phenology in land surface models is crucial for predicting the energy, water, and carbon budgets of these managed ecosystems [*Betts*, 2005; *Lokupitiya et al.*, 2009; *Ma et al.*, 2012]. In regions with large agricultural coverage, a reasonable estimation of crop phenology is especially important in order to simulate the regional thermodynamic properties of the atmospheric boundary layer [*Raddatz and Cummine*, 2003]. In the United States Corn Belt, soybean and corn are cultivated on approximately 600,000 km^2 of the land surface—an area greater than the entire state of California [*Griffis et al.*, 2013]. In order to predict future climate change impacts on the energy, water, and carbon budgets of this region, as well as to estimate the climate impact on food production, models that can simulate crop phenology and growth under typical human management are required.

The Community Land Model (CLM) is the land surface scheme of the Community Earth System Model (CESM) and one of the most widely used land surface schemes in regional and global scale simulations [*Sacks et al.*, 2008; *Lawrence and Chase*, 2009, 2010; *Jin and Miller*, 2010; *Levis*, 2010; *Li and Zhuguo*, 2010; *Gopalakrishnan et al.*, 2011; *Sakaguchi et al.*, 2011; *Lawrence et al.*, 2011, 2012; *Bonan et al.*, 2012; *Levis et al.*, 2012]. Since CLM is part of the Earth system model framework, it is compatible with other modeling components such as regional or global circulation models (i.e., the Weather Research and Forecasting Model and the Community Atmosphere Model) and provides an excellent platform for simulation of land surface processes of various ecosystems, including cropping systems [*Levis et al.*, 2012; *Drewniak et al.*, 2013]. CLM has been evaluated against observations across the globe over different ecosystems [*Kumar and Merwade*, 2011; *Sakaguchi et al.*,

2011; *Wang and Zeng*, 2011; *Yuan and Liang*, 2011]. However, the model has only recently been adapted to include biophysical processes and parameters specific to major cropping systems and has been evaluated against observations at relatively few sites [*Kumar and Merwade*, 2011; *Yuan and Liang*, 2011; *Levis et al*., 2012; *Drewniak et al*., 2013].

The crop simulation in CLM version 3.5 [*Oleson et al*., 2008; *Stöckli et al*., 2008] was prescribed as grasslands (drought-stressed deciduous and unmanaged) to reduce the constraints from limited crop management data and to facilitate simulation of crops under future climate scenarios. The unmanaged cropland in CLM3.5 was found to underestimate leaf area index (LAI; m^2 leaf m^{-2} ground) during the growing season and simulated an unrealistically long growing season into the early winter [*Levis et al*., 2012]. This biased crop phenology propagated into the simulations of surface albedo, soil moisture, and net ecosystem CO_2 exchange (NEE; μmol m^{-2} s^{-1}) [*Levis et al*., 2012]. With this simplified crop parameterization, CLM3.5 was evaluated against 16 AmeriFlux sites. The simulated sensible heat flux (*H*; W m^{-2}) showed good agreement with observations, except at nine crop sites, where CLM3.5 missed the observed two peaks of *H* during the growing season [*Kumar and Merwade*, 2011]. In another study [*Yuan and Liang*, 2011], CLM3.5-simulated daily sensible heat fluxes for two crop sites (AmeriFlux sites ARM and Bo1) were less correlated with the observations (0.50 for ARM and 0.49 for Bo1) compared to the average of 13 nonagricultural sites (0.64) [*Yuan and Liang*, 2011].

In this study we examined two versions of CLM that have cropping schemes (CLM3.5-CornSoy and CLM4-Crop) and tested them against two crop sites over a period of 4 years to evaluate their ability to simulate crop phenology, energy fluxes, and NEE. The first model, CLM3.5-CornSoy, includes phenological processes and parameters specific to corn and soybean ecosystems and simulates prognostic leaf emergence, grain filling, and harvest dates. The second model, CLM4-Crop [*Lawrence et al*., 2012; *Levis et al*., 2012], is able to simulate prognostic corn, soybean, and spring wheat for North America. Both of the crop algorithms were derived from Agro-Integrated Blosphere Simulator (IBIS) [*Kucharik*, 2003], with some key differences that will be described later. Here we evaluate CLM3.5-CornSoy and CLM4-Crop at two agricultural AmeriFlux sites in order to address the following questions: (1) What are the strengths and weaknesses of each model when simulating crop phenology? (2) To what extent do model errors in phenology influence the simulated energy and carbon fluxes? and (3) What are the key model deficiencies that must be addressed in order to reduce model biases in simulating phenology, energy, and carbon fluxes?

2. Methods

2.1. Two Crop-Enabled Models

CLM is the land surface scheme of CESM [*Bonan and Oleson*, 2002; *Zeng et al*., 2002; *Dai et al*., 2003; *Dickinson and Oleson*, 2006; *Oleson et al*., 2008, 2010]. CLM simulates surface albedo; radiation transfer through the canopy; soil, leaf, and canopy air temperature; sensible and latent heat fluxes; and momentum exchange between land and atmosphere in its biogeophysical modules. CLM simulates carbon allocation and transfer between ecosystem carbon pools (plant organs, litter, and soil organic matter) in its biogeochemical modules. In this study, both candidate models were coupled to the CN module [*Thornton et al*., 2007, 2009], which has demonstrated better performance in simulating photosynthesis [*Sakaguchi et al*., 2011].

Two versions of CLM (CLM3.5 and CLM4) are compared in this study. CLM3.5 is a transitional model from the earlier version 3.0 with an improved simulation of the hydrological cycle [*Oleson et al*., 2004a, 2004b, 2007, 2008]. In this study, we added a crop phenology module to CLM3.5-CN. The revised model is called CLM3.5-CornSoy.

CLM4 shares similar biogeophysical and biogeochemical schemes with CLM3.5 but with modifications that have been proved to cause increased soil moisture variability, drier soils, and lower soil temperature in organic-rich soils [*Oleson et al*., 2008]. The major modifications include a revised numerical solution of the Richards equation [*Decker and Zeng*, 2009; *Zeng and Decker*, 2009], a revised ground evaporation scheme [*Sakaguchi and Zeng*, 2009], and a better representation of the hydraulic and thermal properties of organic soils [*Lawrence and Slater*, 2007]. *Levis et al*. [2012] incorporated crop-specific phenology and carbon allocation algorithms into the CLM4.0-CN [*Lawrence et al*., 2012]. The crop plant functional type (PFT) optical properties have been parameterized according to the values presented in *Asner and Wessman* [1998]. This version of the crop simulation-enabled model is called CLM4-Crop.

Table 1. Parameters Used in CLM3.5-CornSoy[a]

	GDT_{on}[b]	GDT_{grain}[c]	*Day_L*[d]	χ_L[e]	F_{LNR}[f]	V_{cmax25}[g]
Corn	**450**	**1105**	**45,000**	−0.30	**0.05**	*50*
Soybean	**400**	**1330**	**40,800**	−0.30	0.10	*50*

[a]New parameters or new values in this study are presented in bold.
[b]Leaf emergence threshold of growing degree time.
[c]Grain fill threshold of growing degree time.
[d]Typical day length when harvest begins in seconds.
[e]Leaf orientation index (−1 for vertical distribution and 1 for horizontal distribution).
[f]Fraction of leaf nitrogen in Rubisco.
[g]Maximum rate of carboxylation at 25°C (μmol CO_2 m^{-2} s^{-1}).

2.1.1. Phenology Schemes

The crop algorithms in CLM3.5-CornSoy are specific to corn and soybean, the dominant crops in the Corn Belt, and were first implemented in Agro-IBIS. Agro-IBIS has been evaluated for North American midlatitude study sites [*Kucharik and Twine*, 2007; *Twine and Kucharik*, 2009]. Two phenological phases of crops are simulated in CLM3.5-CornSoy: phase 1 is from leaf emergence to the beginning of grain fill and phase 2 is from the beginning of grain fill until harvest. Before phase 1 is initiated, CLM3.5-CornSoy calculates the growing degree time ((GDT) or heat unit) and tests if it reaches the leaf emergence threshold (GDT_{on}; Table 1). When GDT exceeds the threshold, leaf emergence occurs, assuming that land managers have already planted their fields. The timing of grain fill is simulated using GDT with a different threshold (GDT_{grain}; Table 1). When the crops reach the grain filling stage, the LAI stops increasing as crops begin to allocate more carbon into the reproduction pool. In CLM3.5-CornSoy, background litter fall was increased in order to represent the reduction of carbon allocated to leaves. Thus, once the grain filling is initiated, LAI will start to decrease slowly. Harvest time is estimated using day length, similar to the way leaf off is simulated for seasonal deciduous trees.

GDT is a thermal time variable similar to growing degree days (GDDs) but calculated on a half hourly model time step:

$$\mathrm{GDT} = \int (\mathrm{T_{air}} - \mathrm{T_{ref}}) \cdot \mathrm{dt}, \ \text{when} \ T_{air} > T_{ref} \tag{1}$$

Here T_{air} is the air temperature at 2 m, and the reference temperature T_{ref} is 8°C.

Compared to GDD, GDT is more sensitive to temperature variations especially in early growing season. For example, during early growing season, some days have several hours above the base temperature, but the daily averaged temperature is below the base temperature. In this case the temperature will accumulate in GDT but not GDD.

The harvest time is estimated using the daytime length *Day_L* as the threshold (Table 1). The process of harvest is simplified as a rapid "litter fall." Currently, this model does not simulate the reproductive carbon pool.

The crop algorithm in CLM4-Crop also originated from the Agro-IBIS model [*Levis et al.*, 2012]. The crop types in CLM4-Crop include corn, soybeans, and temperate midlatitude cereals. In this study, only corn and soybean schemes were tested because they represent the dominant cropping system in the Corn Belt. CLM4-Crop simulates one more phenological phase than does CLM3.5-CornSoy. Phase 1 in CLM4-Crop starts at planting and ends with leaf emergence. Phase 2 and phase 3 are the same as CLM3.5-CornSoy's two phases. In CLM4-Crop, harvest commences automatically when the crops reach physiological maturity, which is defined by a GDD threshold.

Another important difference between the phenology algorithms used in these two models is that CLM4-Crop has a maximum constraint on LAI (5 for corn and 6 for soybean), while CLM3.5-CornSoy does not limit the maximum LAI. The benefit of using a maximum constraint is that the values are guaranteed to fall within a realistic range; however, such approaches are not physically based and can result in a loss of information such as masking of interannual variations in maximum LAI values.

2.1.2. Crop Parameterization in the Two Models

Two other modifications to CLM3.5 were made to better simulate corn and soybean systems. In the original model, there was a nitrogen limitation in place for all plant functional types. Here we assume that nitrogen is

not limiting, since for corn, it is typically applied according to guidelines developed in each state through N rate experiments by Extension Service scientists. "Safety" factors are typically built into these guidelines to virtually ensure that N will not be yield limiting. Soybeans are legumes that derive their N from symbiotic bacteria. Thus, the nitrogen limitation in the original CLM3.5-CN was removed for corn and soybean. The same approach is used in CLM4-Crop, with the nitrogen limitation disabled for corn, soybean, and temperate cereals [*Levis et al*., 2012]. The second change we made was only for corn. The fraction of leaf nitrogen in Rubisco was modified from 0.1 to 0.05 according to previous studies on C_4 plants [*Schmitt and Edwards*, 1981; *Rowan et al*., 1987; *Makino et al*., 2003]. This modification was made to prevent unrealistically high photosynthetic rates.

In CLM4-Crop, the maximal carboxylation rate at 25°C (V_{cmax25}) was set to 101 μmol CO_2 m^{-2} s^{-1} for corn, soybean, and temperate cereals according to measured values for C_3 crops [*Kattge et al*., 2009], compared to 50 μmol CO_2 m^{-2} s^{-1} in CLM3.5-CornSoy [*Wullschleger*, 1993; *Kucharik et al*., 2000; *Oleson et al*., 2007] (Table 1).

In CLM3.5-CornSoy, the leaf orientation index for corn and soybean is −0.3 (Table 1), which was adopted from the Simple Biosphere Model [*Dorman and Sellers*, 1989]. The leaf orientation index describes the departure of leaf angles from a random distribution and equals +1 for horizontal leaves, 0 for random leaves, and −1 for vertical leaves. In CLM4-Crop, the leaf orientation index for corn and soybean was set to the more vertical orientation of −0.5 according to the Agro-IBIS values [*Levis et al*., 2012]. A detailed list of CLM4-Crop parameter values can be found in *Levis et al*. [2012].

2.1.3. The Water Stress Factor

Both CLM3.5 and CLM4 use a PFT-dependent water stress factor to describe the soil water constraint on the transpiration or photosynthetic rate. This water stress factor is calculated as

$$\beta_t = \sum_i w_i r_i \tag{2}$$

where w_i is a plant wilting factor for layer i and r_i is the fraction of roots in layer i. Currently, both models use a static root distribution function to describe all crop PFTs. The plant wilting factor is then calculated according to the soil water matric potential [*Oleson et al*., 2004b, 2010]. Here the soil layer needs to be hydrologically active, and in CLM4, this is defined as the upper 10 of the total 15 soil layers.

2.2. Model Spin-Up

During spin-up, CLM3.5-CornSoy and CLM4-Crop were run offline and driven by the Princeton meteorological forcing data set [*Sheffield et al*., 2006]. The data ranged from 1948 to 2008. The spatial and temporal resolution was 1 × 1° and 3 h, respectively. The meteorological fields include solar radiation, air temperature, air humidity, air pressure, wind speed, and precipitation. To ensure that the models reached a steady state (i.e., that the slowest soil storage pools of carbon had reached equilibrium), we recycled the forcing data for 4000 years for CLM3.5-CornSoy and 1000 years for CLM4-Crop [*Thornton and Rosenbloom*, 2005; *Sakaguchi et al*., 2011]. After spin-up, the soil organic carbon of the field reached a steady state value of 20.6 and 11.2 kg C m^{-2} in CLM3.5-CornSoy and 21.7 and 10.1 kg C m^{-2} in CLM4-Crop for corn and soybean, respectively. These values are in close agreement with the National Cooperative Soil Survey values (14.2 to 22.7 kg C m^{-2}).

2.3. Research Sites

The AmeriFlux sites US-Ro1 and US-Ro3 are located approximately 25 km to the south of Minneapolis/St. Paul (44°41′19″N, 93°4′22″W; 259.7 m above sea level). The two sites are about 500 m apart, with US-Ro3 in the north and US-Ro1 in the south. Both sites are rain-fed rotation fields of corn (*Zea mays*) and soybean (*Glycine max*). Waukegan silt loam (fine, mixed, and mesic typic hapludoll) is the major soil type in these two fields with a surface layer of high organic carbon content (2.6% average) and variable thickness (0.3–2.0 m) underlain by coarse glacial outwash sand and gravel with little water-holding capacity. The average air temperature from 1980 to 2010 was 7.8°C with a maximum annual mean temperature of 13.0°C. The annual average precipitation for the same period was 814 mm. One major difference between the two sites is that US-Ro1 is under conventional management and US-Ro3 is managed under reduced tillage with winter cover crops [*Baker and Griffis*, 2005]. These site differences, with near-identical meteorology, provide a good opportunity to evaluate the robustness of the crop scheme implemented in CLM. At site US-Ro1, corn

was grown in 2007 and 2009, and soybean was grown in 2008 and 2010. At site US-Ro3, corn was grown in 2007, 2008, and 2010, and soybean was grown in 2009. These 8 years of site data were used to test the CLM3.5-CornSoy and CLM4-Crop simulations.

2.4. Contemporary Meteorological Forcing Data

The meteorological forcing data were averaged over the two sites (approximately 500 m apart from each other) for every hour to get an ensemble forcing data set from 2007 to 2010. Data used to drive the model included solar radiation (Eppley Precision Spectral Pyranometer, The Eppley Laboratory, Newport, RI, USA), air temperature and humidity (HMP 35C, Vaisala Inc., MA, USA), air pressure, wind speed (CSAT3, Campbell Scientific, Inc., UT, USA), and precipitation. Precipitation was measured using two instruments, a tipping bucket rain gauge (6028-B, All Weather Inc., CA, USA) with a precision of 0.25 mm for liquid precipitation and a weighing rain gauge (Geonor T-200B, Campbell Scientific, Inc., UT, USA) for solid precipitation. We did not use the tipping bucket rain gauges in the winter because they are known to systematically underestimate snowfall [*Groisman and Legates*, 1994; *Upton and Rahimi*, 2003]. The time attribution of the local measured meteorological data is converted from local time to the Greenwich mean time to be consistent with CESM.

2.5. Model Evaluation Data

LAI was measured approximately once a week with an AccuPAR hand-held sensor (AccuPAR, Mode PAR-80, Decagon Devices Inc., Pullman, WA, USA). Eddy covariance (EC) measurements of sensible heat flux (H; W m^{-2}), latent heat flux (LE; W m^{-2}), and net ecosystem CO_2 exchange (NEE; μmol m^{-2} s^{-1}) have been ongoing at these two sites since 2004 [*Baker and Griffis*, 2005]. These fluxes were quality controlled and filtered using a friction velocity (u_*) threshold greater than 0.1 m s^{-1} (a typical value for agricultural land) to eliminate periods of weak turbulence and were gap filled. Systematic errors in EC-measured H and LE due to a lack of energy balance closure were corrected by assuming the available energy (the residual of the net radiation minus the ground heat flux), and the Bowen ratio were measured correctly. H and LE were proportionaly increased for each half hourly period to force energy balance closure [*Blanken et al*., 1997; *Xiao et al*., 2010]. Soil heat flux (G) at the surface was estimated by correcting the measured heat flux at a soil depth of 10 cm (HFP01SC, Hukseflux USA, Inc., NY, USA) using the calorimetric method. The required soil temperature measurements were made using thermocouples positioned above (but offset from) the heat flux plates. Other details regarding the EC measurements, data processing, and data quality assessment can be found in previous studies [*Baker and Griffis*, 2005; *Griffis et al*., 2005].

The EC-measured NEE was partitioned into gross primary production (GPP) and ecosystem respiration (ER) using the Fluxnet Canada methodology described by *Barr et al*. [2004]. The grain yield for each site was recorded by the Rosemount Research and Outreach Center at the University of Minnesota. Using the laboratory-measured mean grain carbon content (45% for corn and 54% for soybean), we calculated the carbon lost through harvest each year [*Baker and Griffis*, 2005]. In order to close the annual carbon budget for cropping systems, we have estimated the net biome productivity (NBP) by adding the harvested grain carbon (a carbon loss) to the EC-measured annual NEE:

$$\mathrm{NBP} = \mathrm{NEE} + C_{\mathrm{grain}} \tag{3}$$

where C_{grain} is the harvested grain carbon calculated from the yield data at the sites.

2.6. Evaluation of Model Performance

In our simulations, only one crop is growing in the entire grid cell. No other PFTs are growing in the grid cell. The footprint of the NEE measurement is also within the field. Thus, we can compare the measured and simulated fluxes.

The metrics used for evaluating model performance were the correlation coefficient and bias.

The correlation coefficient (r) of a variable X was calculated as

$$r = \frac{\sum_{i-1}^{n}\left(X_{mi} - \overline{X_m}\right)\left(X_{oi} - \overline{X_o}\right)}{\sqrt{\sum_{i-1}^{n}\left(X_{mi} - \overline{X_m}\right)}\sqrt{\sum_{i-1}^{n}\left(X_{oi} - \overline{X_o}\right)}} \tag{4}$$

where X_m and X_o are the modeled and observed values, respectively, and the overbars represent the means.

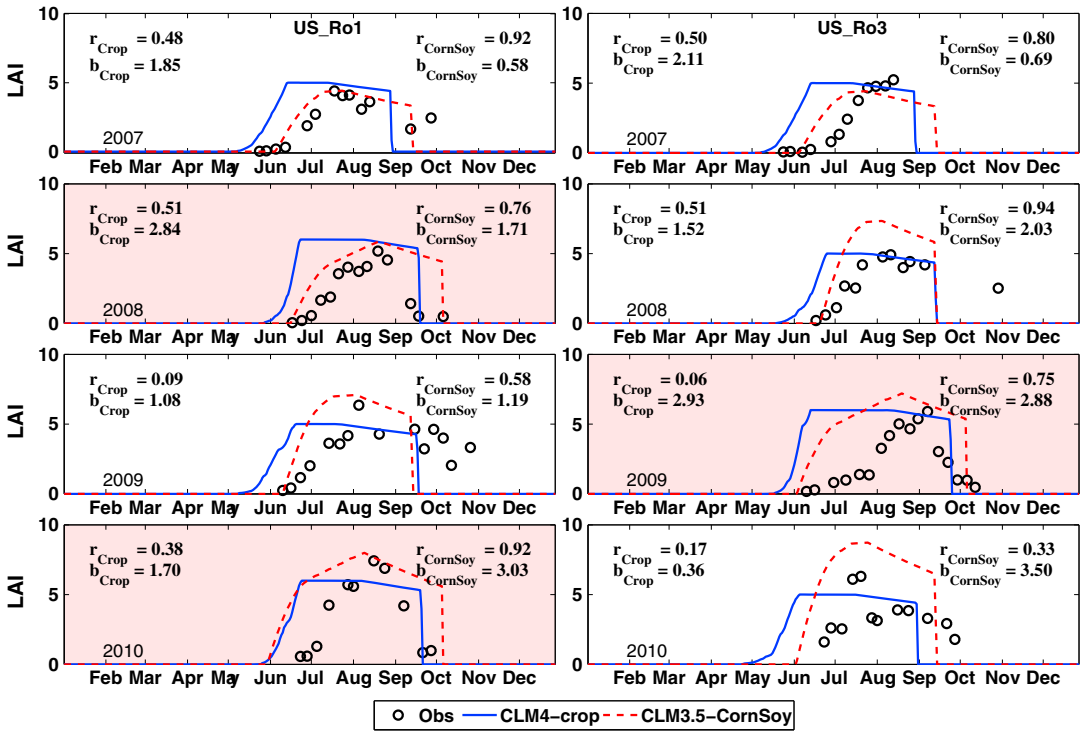

Figure 1. Simulated LAI compared with field observations. The circles represent the observed values. The red line represents CLM3.5-CornSoy, and the blue line represents CLM4-Crop. The white backgrounds represent corn years, and the shaded background represents soybean years. The correlation coefficients (*r*) and bias (*b*) are calculated based on weekly averaged values. The subscript Crop stands for CLM-Crop, and CornSoy stands for CLM3.5-CornSoy.

Model bias was calculated as the mean of the model observation residuals [*Schaefer et al.*, 2012]:

$$b = \overline{(X_{mi} - X_{oi})} \tag{5}$$

A positive bias indicates that the model overestimated the observations.

The ideal model will have $r = 1$ and $b = 0$. If the modeled values yield a correlation coefficient close to 1, but a large bias, we can conclude that the model has captured the dynamics of the processes but that relevant parameter values need further optimization. If the modeled values yield a bias close to 0, but a low correlation coefficient with the observations, we can conclude that the model does not adequately capture the dynamics of the processes. In this situation, a more realistic mechanism needs to be developed to improve the simulation.

3. Results and Discussion

3.1. Phenology

The seasonal patterns of LAI are provided in Figure 1. The correlation coefficient between simulated and observed corn LAIs for CLM3.5-CornSoy was 0.71 ($b = 1.60$) and 0.81 ($b = 2.54$) for soybean. CLM4-Crop simulations yielded LAI correlation coefficients of 0.35 ($b = 1.39$) for corn and 0.22 ($b = 2.71$) for soybean. Overall, both models overestimated LAI during the growing season. The CLM4-Crop-simulated LAI was less correlated with the observations because of unrealistically high LAI values during the early growing season in all modeled years. This overestimated LAI in the early growing season in CLM4-Crop was also observed in previous studies [*Levis et al.*, 2012; *Drewniak et al.*, 2013], where they suggested that the planting date was biased earlier. In this study, CLM4-Crop-predicted planting dates were within 10 days of the actual planting dates. Thus, the timing of leaf emergence seems to be predicted early after planting in CLM4-Crop. Further, it is likely that using the observed crop V_{cmax25} value of 101 μmol CO_2 m^{-2} s^{-1} in the present canopy radiative transfer scheme also contributed to the amplified growth rate. *Bonan et al.* [2012] found that the use of leaf level-measured values of V_{cmax25} within the sunlit-shaded big-leaf framework of CLM resulted in higher photosynthetic rates when nitrogen was nonlimiting (i.e., for cropping systems). Although currently CLM4-Crop uses the maximum LAI constraint to limit corn and soybean LAI under 5 and 6, respectively, this early growing season offset

Table 2. Growing Season (May to September) Correlation Coefficients and Bias (W m^{-2}, in Parenthesis) of the Two Model-Simulated Hourly Net Radiation (R_n), Sensible Heat Flux (H), Latent Heat Flux (LE), Ground Heat Flux (G), and Leaf Temperature (T_v)[a]

Year	Crop	R_n		H		LE		G		T_v	
		CLM3.5-CornSoy	CLM4-Crop	CLM3.5-CornSoy	CLM4-Crop	CLM3.5-CornSoy	CLM4-Crop	CLM3.5-CornSoy	CLM4-Crop	CLM3.5-CornSoy	CLM4-Crop
US-Ro1											
2007	corn	0.98 (12.3)	0.98 (12.7)	0.62 (−34.2)	0.65 (5.9)	0.90 (9.2)	0.81 (−26.6)	0.50 (6.5)	0.49 (4.4)	0.90 (−0.9)	0.91 (0.2)
2008	soybean	0.98 (21.5)	0.98 (21.5)	0.74 (−25.9)	0.47 (−2.8)	0.75 (−5.8)	0.52 (−11.1)	0.39 (9.0)	0.49 (1.3)	0.93 (0.2)	0.89 (1.0)
2009	corn	0.98 (12.8)	0.92 (18.0)	0.80 (−35.1)	0.52 (−2.0)	0.86 (−1.6)	0.65 (−23.2)	0.37 (7.3)	0.41 (4.6)	0.86 (−0.1)	0.86 (0.6)
2010	soybean	0.98 (26.2)	0.98 (31.0)	0.54 (20.5)	0.56 (18.6)	0.85 (29.3)	0.86 (−16.5)	0.31 (−12.5)	0.30 (−16.6)	0.89 (−0.2)	0.94 (0.4)
US_Ro3											
2007	corn	0.99 (−0.4)	0.98 (−0.1)	0.68 (−43.5)	0.72 (−3.2)	0.91 (12.3)	0.83 (−24.0)	0.50 (8.3)	0.48 (6.2)	0.93 (−0.8)	0.93 (0.3)
2008	corn	0.99 (5.7)	0.98 (9.0)	0.73 (−36.2)	0.76 (10.9)	0.86 (13.3)	0.80 (−30.5)	0.54 (9.1)	0.51 (1.3)	0.92 (−0.2)	0.94 (1.5)
2009	soybean	0.98 (5.1)	0.93 (4.3)	0.83 (−24.3)	0.54 (8.5)	0.90 (5.4)	0.67 (−18.1)	0.5 (6.7)	0.55 (0.1)	0.92 (−0.1)	0.89 (0.7)
2010	corn	0.99 (2.9)	0.98 (6.0)	0.69 (−8.2)	0.55 (22.2)	0.92 (7.1)	0.85 (−32.4)	0.64 (3.8)	0.64 (2.8)	0.92 (−0.2)	0.92 (0.7)
Average											
Corn		0.99(6.7)	0.97 (9.1)	0.70 (−31.4)	0.64 (6.8)	0.89(8.1)	0.79 (−27.3)	0.51 (7.0)	0.51 (3.9)	0.91 (−0.4)	0.91 (0.7)
Soybean		0.98 (17.6)	0.96 (18.9)	0.70 (−9.9)	0.52 (8.1)	0.83 (9.6)	0.68 (−15.2)	0.40 (1.1)	0.45 (−5.1)	0.91 (−0.0)	0.91 (0.7)
All		0.98 (10.8)	0.97 (12.8)	0.70 (−23.4)	0.60 (7.3)	0.87 (8.7)	0.75 (−22.8)	0.47 (4.8)	0.48 (0.5)	0.91 (−0.3)	0.91 (0.7)

[a]All p values are ≤ 0.01.

represents an important model bias that propagates into energy and carbon flux simulations that needs to be corrected.

Compared to CLM4-Crop, CLM3.5-CornSoy displayed more year-to-year LAI variability. For example, in 2007, the U.S. Drought Monitor classified the study region in the moderate drought category due to below normal rainfall in June and July. This caused a significant depletion of soil water content. This phenomenon was captured by CLM3.5-CornSoy as a lower maximum LAI for 2007 than other years for both corn and soybean (maximum LAI of corn for 2007 was about 5, while in other corn years, it reached 7 to 8). CLM4-Crop did not capture this interannual variability because the simulated LAI reached the model's maximum LAI limit every year (Figure 1). On the other hand, CLM3.5-CornSoy overestimated corn maximum LAI in 2008 and 2010 by 2. These uncertainties are diagnosed further in section 3.3.

Both models predicted the timing of grain filling (peak LAI) very well for all years. The harvest dates were simulated earlier than the real harvest dates in both models. This is because in the model, harvest happens when the crops reached physiological maturity, and in practice, farmers often delay harvest to allow the grain to dry in the field (e.g., moisture content lower than 20%) to minimize or eliminate fossil fuel-based drying prior to storage or shipping. The simulated harvest date was usually in September, while the actual corn and soybean harvest in the Upper Midwest typically occurs from late October to mid-November.

The overall need to improve the understanding of environmental controls on vegetation phenology was highlighted by *Richardson et al.* [2012]. They examined the simulation of phenology in 14 land surface schemes at 10 forested sites. Their results indicate that it is a major challenge for state-of-the-art models to predict how phenology responds to future climate change. For example, simulations of deciduous forest phenology misrepresent the critical transition periods in nearly all cases. They found that the simulations were biased with longer growing seasons and overestimation of gross ecosystem photosynthesis by $+160 \pm 145$ g C m^{-2} yr^{-1} in spring and $+75 \pm 130$ g C m^{-2} yr^{-1} in fall. In the next sections, we examine the extent to which bias in crop phenological simulation impacts the energy and carbon flux simulations.

3.2. Energy Fluxes

The two models share identical schemes for simulating the energy balance. All of the energy flux-related differences we report in this section can be attributed to the differences in phenological and hydrological schemes, as well as the different parameterizations in crop optical properties.

The modeled hourly net radiation (R_n) was highly correlated with the observations ($r > 0.92$) but was slightly overestimated by both models (Table 2). The averaged CLM3.5-CornSoy R_n bias was 6.7 W m^{-2} for corn and 17.6 W m^{-2} for soybean. The averaged CLM4-Crop R_n bias was 9.1 W m^{-2} for corn and 18.9 W m^{-2} for soybean. Further, the simulated R_n was consistently biased higher for the soybean canopy than for the corn canopy in both models. There are two major differences in the parameterization of crop leaf optical properties in the two models. First, CLM4-Crop defines a more vertically oriented leaf distribution adopted from Agro-IBIS than CLM3.5-CornSoy (see section 2.1.2). Leaf orientation depends on species and can vary as a function of season (phenology) [*Ross*, 1975]. *Ross and Ross* [1969] provided leaf angle distribution formulae and summarized data for the leaf angle distribution factor for different crops. The value for corn ranged from −0.13 to 0.46. The authors did not report parameter values for soybean. Instead, they provided estimates for another bean crop (*Vicia faba*) that ranged from 0.30 to 0.39 [*Ross and Ross*, 1969; *Ross*, 1975]. The CLM3.5-CornSoy leaf angle distribution factor of −0.3 and the CLM4-Crop leaf angle distribution factor of −0.5 for crops are too vertical compared to these observations. Our field data and analyses [*Baker and Griffis*, 2008, 2012] show that both corn and soybean leaves have a close to spherical distribution but more horizontal than vertical (see Figures S1 and S2 in the supporting information). The typical leaf angle distribution factors at our sites from leaf emergence to grain fill (maximum LAI) and from grain fill to harvest are 0.17 and 0.12 for corn and 0.17 and 0.18 for soybean. Our sensitivity tests indicate that the more horizontal distribution will amplify the net radiation bias. The parameterization schemes for the optical properties of crops are different in the two models. CLM3.5-CornSoy adopted parameters of crop leaf and stem reflectance, transmittance from *Dorman and Sellers* [1989]. CLM4-Crop uses parameters from *Asner and Wessman* [1998], which have a significantly lower reflectance and higher transmittance for crops. That partly explains why CLM4-Crop has higher net radiation simulated for both crops. However, the parameters used in CLM4-Crop are closer to the documented values in previous studies [*Walter-Shea et al*., 1989; *Walter-Shea and Norman*, 1991; *Schepers et al*., 1996]. Thus, we examined the monthly bias of R_n and LAI. The linear regression showed positive correlations between monthly LAI bias and monthly net daytime and nighttime long-wave radiation biases ($r^2 = 0.20$ and 0.36, respectively; both p values are less than 0.01, see Figures S3 and S4 in the supporting information). These analyses indicate that high LAI is associated with a lower canopy temperature and therefore less outgoing long-wave radiation, both during daytime and nighttime. These results highlight that in order to improve the R_n bias, a better crop phenology (LAI) simulation is needed. This is a challenging task because of the feedback among LAI, radiation balance, photosynthesis, and leaf growth.

Although the total energy received by the canopy only had a bias within 20 W m^{-2}, there were important deficiencies when partitioning the total energy into *H*, *LE*, and *G*.

CLM4-Crop exhibited less bias in simulated *H* than CLM3.5-CornSoy. The correlation coefficient for *H* between CLM4-Crop simulation and observation was 0.64 ($b = 6.8$ W m^{-2}) for corn and 0.52 ($b = 8.1$ W m^{-2}) for soybean. For CLM3.5-CornSoy, the correlation coefficient for *H* was 0.70 ($b = -31.4$ W m^{-2}) for corn and 0.70 ($b = -9.9$ W m^{-2}) for soybean. The monthly averaged biases of *H* simulations for corn and soybean are shown in Figure 2. Both models underestimated *H* (−40 to −60 W m^{-2}) in May. During the midgrowing season (July and August), *H* was generally overestimated by both models (Figures 2b–2d), except for corn in CLM3.5-CornSoy (Figure 2a). CLM4-Crop showed more pronounced high bias of *H* during midgrowing season for both crops. This indicates that CLM4-Crop likely overestimated leaf temperature during the midgrowing season. The leaf temperature data in Table 2 show that this was the case. This bias is examined further below by considering the model *LE* simulations.

CLM3.5-CornSoy performed slightly better in simulating *LE*. The correlation coefficient between simulated and observed corn *LE* was 0.89 ($b = 8.1$ W m^{-2}) for CLM3.5-CornSoy and 0.83 ($b = 9.6$ W m^{-2}) for soybean. CLM4-Crop simulations gave an *LE* correlation coefficient of 0.79 ($b = -27.3$ W m^{-2}) for corn and 0.68 ($b = -15.2$ W m^{-2}) for soybean. These results indicated that *LE* was overall underestimated for both corn and

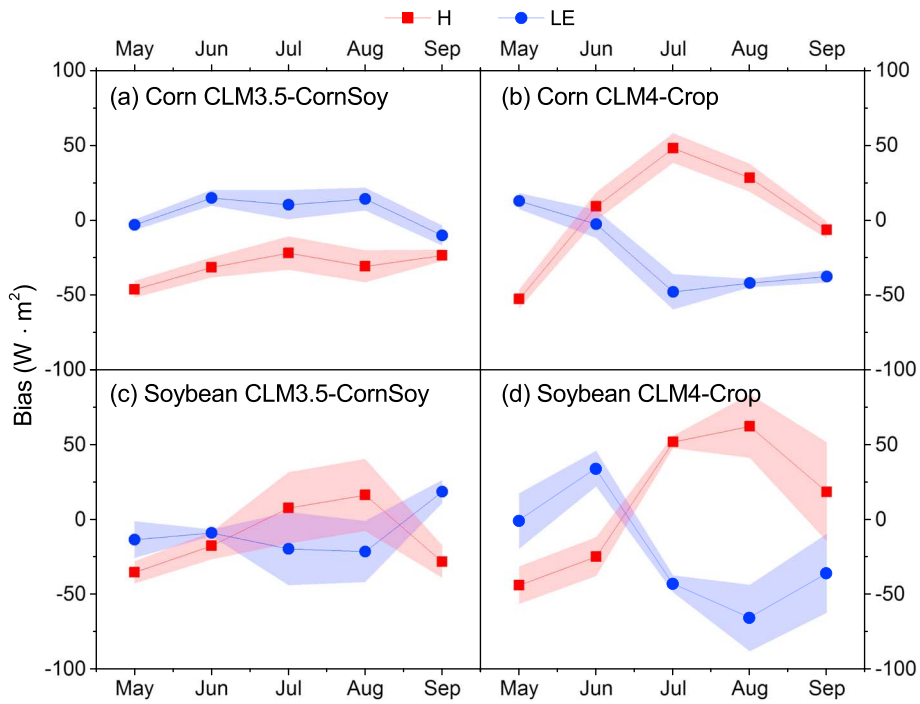

Figure 2. (a–d) The 2007–2010 monthly average bias (model-observation) of the two model-simulated *H* and *LE*. For corn, it is averaged over five model years. For soybean, it is averaged over three model years. The shaded regions represent the standard errors of the monthly biases.

soybean by CLM4-Crop. This *LE* deficiency is pronounced during middle and late growing season (July to September) when transpiration becomes a major fraction of evapotranspiration (Figure 2).

To determine what caused the underestimation of *LE* and the overestimation of *H* from July to September in CLM4-Crop, we examined the soil water content (SWC) along with the root distribution for crops (Figure 3). The trends are the same in all years. As an example, Figure 3 shows the evaluation of SWC in 2008 at site US-Ro1. CLM3.5-CornSoy and CLM4-Crop performed similarly when simulating SWC in layers above −5 cm and −15 cm. The amplitude of interannual SWC variation was captured well to the depth of −15 cm; however, both models have a slightly earlier (about 7 days) onset of SWC increase caused by earlier snowmelt. CLM4-Crop overestimated SWC at depth of 5 cm from mid-April to late June by about 10%. From July to September, CLM4-Crop underestimated SWC in all layers. The most pronounced underestimation (around 20%) is from −15 cm to −50 cm, where most of the crop roots are located. CLM3.5-CornSoy also underestimated SWC from −5 cm to −50 cm during this period, with the amplitude less than CLM4-Crop (around 10%). At the depth of −100 cm, CLM3.5-CornSoy simulated a wetter soil than observed. In contrast, CLM4-Crop simulated a much drier soil than observed (SWC close to 0). The simulated drier soil in CLM4-Crop led to a higher than normal water stress, which was calculated in the model as a smaller β_t (see section 2.1.3). This biased water stress factor further constrains transpiration and caused the underestimation of *LE* in CLM4-Crop. Overall, both models significantly underestimated SWC (around 20%) during midgrowing season at soil layers above −50 cm, and CLM4-Crop underestimated SWC to the depth of 100 cm. Therefore, additional work is needed to improve soil water dynamics especially at deeper soil layers. Further, when calculating water stress for crops, a reasonable root distribution is very important. Currently in both models, the root distribution for all crop PFTs is a static equation, and the roots in CLM4-Crop are distributed toward shallower soil than CLM3.5-CornSoy. Root distribution can vary substantially depending on soil type, soil water availability, crop type, and other management factors like tillage and fertilization. Maximum rooting depths, reported in previous studies ranged from 90 to 240 cm and 70 to 180 cm for corn and soybean, respectively [*Allmaras et al.*, 1973; *Dwyer et al.*, 1988; *Keller and Bliesner*, 1990; *Laboski et al.*, 1998]. *Drewniak et al.* [2013] incorporated a dynamic rooting scheme into CLM4-Crop to estimate plant root growth and response to environmental conditions. A similar approach could improve the SWC simulation and biases associated with crop water stress.

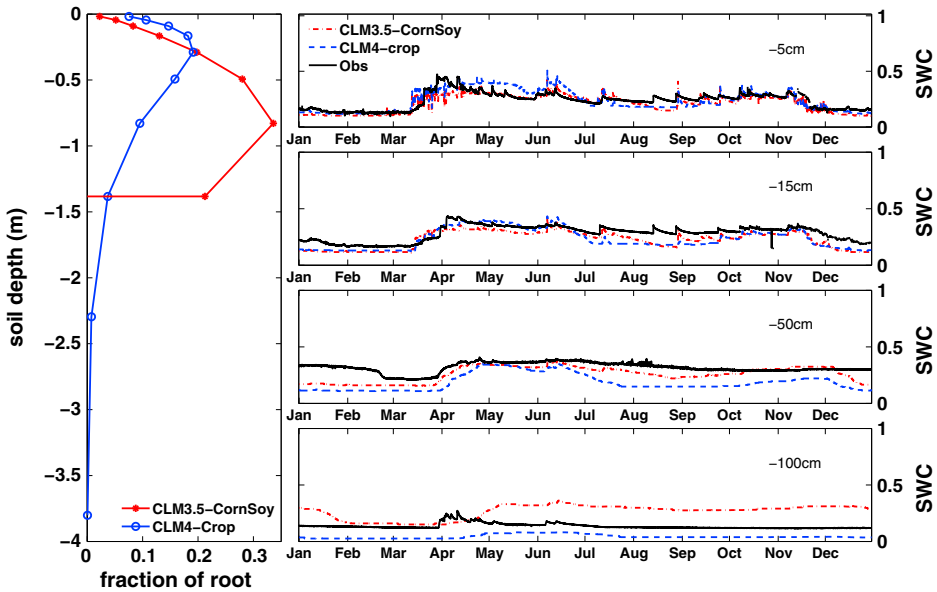

Figure 3. Crop root distribution and evaluation of soil liquid water content simulations at different soil depths in 2008, site US-Ro1, which was in a soybean phase. CLM-simulated soil water contents are linearly interpolated to the observation depths −5 cm, −15 cm, −50 cm, and −100 cm.

The simulated *G* had the lowest correlation with observations (0.30–0.64) of all energy fluxes. Since *G* is calculated as the residual of the surface energy balance in both models, errors in *H* and *LE* propagate into *G*. *G* was biased high in almost all years for both models (Figure 4 as an example), indicating that the simulated sums of *H* and *LE* were biased low. In a number of previous studies, eddy covariance measurements of *H* and *LE* were directly used in model parameterization and evaluations [*Stöckli et al.*, 2008] before energy balance closure corrections were applied. Eddy covariance-measured *H* and *LE* typically represent about 80% of the available energy ($R_n - G$) [*Wilson et al.*, 2002], so parameterizing the model in this way might result in systematically underestimated sum of *H* and *LE*. This may be one reason contributing to the large bias in *G*. Other energy storage terms (i.e., canopy storage and photosynthesis) that have not been explicitly calculated for this comparison may also contribute to the bias, but these terms are expected to be relatively small for corn and soybean.

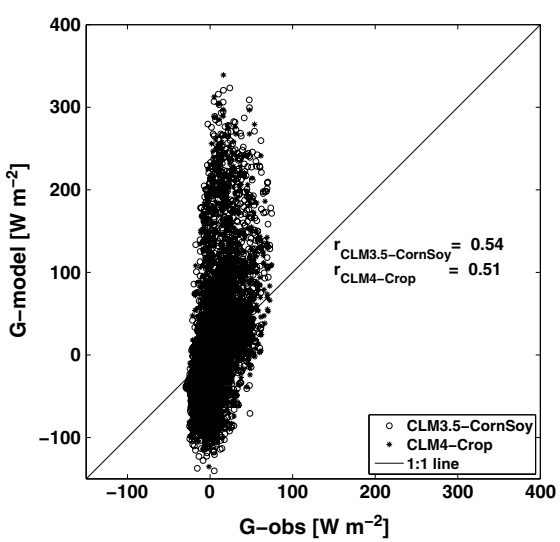

Figure 4. Evaluation of model-simulated *G*. The data used in this figure are from US-Ro3 in 2008, which was in the corn phase of the crop rotation.

3.3. Carbon Fluxes

Overall, both models simulated the amplitude of seasonal NEE reasonably well (Table 3). The average correlation coefficients were 0.87, 0.88, and 0.59 for NEE, GPP, and ER for CLM3.5-CornSoy and 0.55, 0.68, and 0.29 for CLM4-Crop. The lower correlation coefficients for CLM4-Crop were due to three reasons:

First, the accuracy of the NEE and GPP simulations is intimately connected to the phenology simulations. The overestimated LAI during the early growing season in CLM4-Crop led to positive NEE and GPP biases during this period. From May to June, CLM3.5-CornSoy performed better at simulating GPP ($r = 0.93$, $b = 3.73\ \mu\text{mol m}^{-2}\,\text{s}^{-1}$) and NEE ($r = 0.83$, $b = -1.18\ \mu\text{mol m}^{-2}\,\text{s}^{-1}$). CLM4-Crop always

Table 3. Correlation Coefficients and Bias ($\mu mol\ m^{-2}\ s^{-1}$, in Parenthesis) of the Two Model-Simulated Hourly Net Ecosystem Exchange (NEE), Gross Primary Production (GPP), and Ecosystem Respiration (ER)[a]

		NEE		GPP		ER	
Year	Crop	CLM3.5-CornSoy	CLM4-Crop	CLM3.5-CornSoy	CLM4-Crop	CLM3.5-CornSoy	CLM4-Crop
US-Ro1							
2007	Corn	0.89 (−2.8)	0.59 (−0.5)	0.91 (6.0)	0.68 (2.2)	0.54 (3.1)	0.35 (1.7)
2008	Soybean	0.92 (−3.0)	0.70 (−1.4)	0.92 (6.2)	0.75 (3.3)	0.58 (3.1)	0.52 (1.9)
2009	Corn	0.85 (−2.5)	0.48 (−2.0)	0.85 (3.2)	0.47 (3.5)	0.51 (0.6)	0.12 (1.4)
2010	Soybean	0.89 (−0.9)	0.66 (1.6)	0.91 (8.0)	0.82 (3.5)	0.72 (7.1)	0.28 (5.1)
US_Ro3							
2007	Corn	0.89 (−3.0)	0.66 (−0.7)	0.92 (5.5)	0.75 (1.8)	0.62 (2.4)	0.39 (1.0)
2008	Corn	0.82 (−2.0)	0.35 (−0.8)	0.83 (2.8)	0.41 (4.0)	0.54 (0.7)	0.23 (3.1)
2009	Soybean	0.90 (−1.1)	0.73 (−0.8)	0.90 (5.8)	0.74 (2.4)	0.46 (4.6)	0.37 (1.6)
2010	Corn	0.77 (−1.8)	0.27 (−3.1)	0.79 (3.0)	0.81 (6.9)	0.71 (1.1)	0.04 (3.7)
Average							
Corn		0.84 (−2.4)	0.47 (−1.4)	0.86 (4.1)	0.62 (3.7)	0.59 (1.6)	0.23 (2.2)
Soybean		0.90 (−1.7)	0.69 (−0.2)	0.91 (6.7)	0.77 (3.1)	0.59 (4.9)	0.39 (2.8)
All		0.87 (−2.2)	0.55 (−1.0)	0.88 (5.1)	0.68 (3.4)	0.59 (2.9)	0.29 (2.4)

[a]All p values are ≤ 0.01.

overestimated GPP ($r = 0.77$, $b = 8.25\ \mu mol\ m^{-2}\ s^{-1}$) and underestimated NEE ($r = 0.66$, $b = -6.44\ \mu mol\ m^{-2}\ s^{-1}$) for all modeled early growing seasons due to its overestimated early growing season LAI.

Second, the approach adopted by CLM4-Crop to account for the carbon flux (loss) associated with harvested grain is to "dump" the harvested biomass into the litter pool within a single time step. This obviously results in an unrealistic CO_2 emission when compared to the observations and thus lower correlations between the EC measured and modeled NEE and ER. However, for a global simulation, using this approach over the long term is a valid assumption and closes the carbon budget. For CLM3.5-CornSoy, this simplified model only considers crop phenology, and there is no reproductive carbon pool currently. Thus, CLM3.5-CornSoy does not simulate the decomposition of the harvested grain carbon; it only simulates the decomposition of the aboveground biomass as litter fall, and the result agrees well with the EC measurement.

Third, unrealistic water stress in CLM4-Crop caused biased GPP for soybean. CLM4-Crop captured some of the water stress events for corn, when the GPP of corn was reduced due to limited soil water (Figure 5b). However, for soybean, the CLM4-Crop simulations were too sensitive to soil moisture. GPP was overestimated when there was sufficient SWC and underestimated when there was a deficiency in SWC. This simulation problem arises from the bias in soil water content (i.e., too dry for all of the soil layers during midgrowing and late growing season) simulated in CLM4-Crop that led to an overestimation of water stress in July, August, and September. CLM3.5-CornSoy performed better at simulating both GPP and ER for soybean.

CLM4-Crop did a better job of simulating the amplitude of GPP for the corn years largely due to its restriction of maximum LAI. Although CLM3.5-CornSoy performed well in simulating the seasonal pattern of GPP, the maximum values of GPP for corn were significantly overestimated (Figure 5b) due to high bias in LAI during late growing season (Figure 1). Currently, the assumption of no nitrogen limitation all year round for crops might need further investigation. Since growth respiration was calculated in CLM as a fraction of GPP, ER was also overestimated in CLM3.5-CornSoy for corn, which offsets GPP in simulating a reasonable corn NEE in CLM3.5-CornSoy. For soybean, CLM3.5-CornSoy captured the timing of leaf emergence and grain filling very well. The peak GPP was also captured by the model, but GPP during early and late growing season was overestimated. This indicated that the model had a good estimation of the photosynthesis rate during peak season, but one single value of V_{cmax25} is not suitable for early and late growing season. In the newly released CLM version 4.5, a day length-dependent V_{cmax25} was introduced to include the seasonal variation of V_{cmax25} [*Bonan et al.*, 2012; *Oleson et al.*, 2013]. The upscaling of photosynthesis from leaf level to canopy level was also improved by considering the change of V_{cmax25} with depth in the canopy. This change has the potential to improve the early growing season bias of GPP simulated by CLM4-Crop.

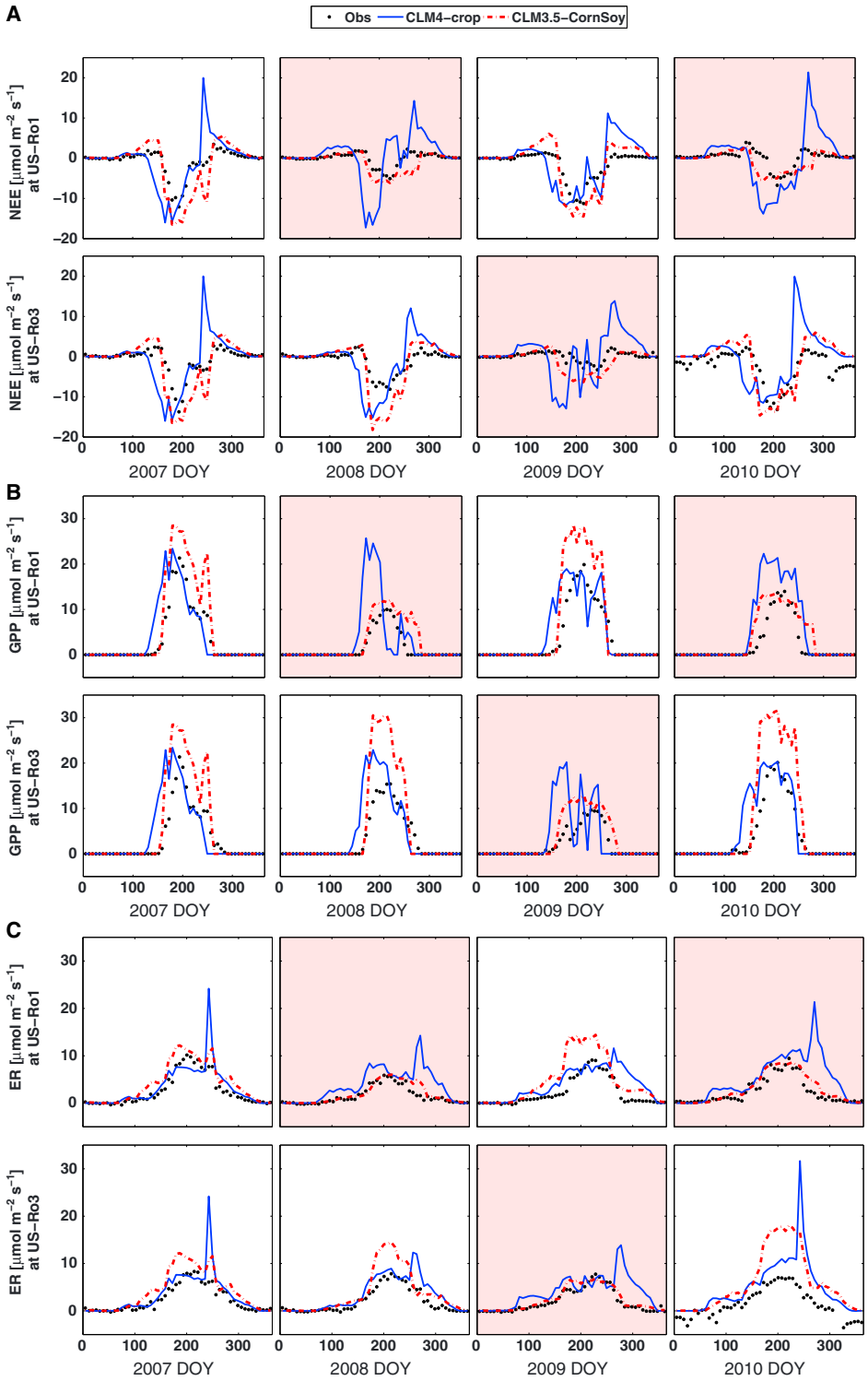

Figure 5. (a) Weekly averaged NEE at the two sites from 2007 to 2010. The white backgrounds represent corn years, and the shaded background represents soybean years. The red dashed lines represent CLM3.5-CornSoy, the blue solid lines represent CLM4-Crop, and the black dots represent observations. (b) Weekly averaged GPP at the two sites from 2007 to 2010. The white backgrounds represent corn years, and the shaded background represents soybean years. The red dashed lines represent CLM3.5-CornSoy, the blue solid lines represent CLM4-Crop, and the black dots represent observations. (c) Weekly averaged ER at the two sites from 2007 to 2010. The white backgrounds represent corn years, and the shaded background represents soybean years. The red dashed lines represent CLM3.5-CornSoy, the blue solid lines represent CLM4-Crop, and the black dots represent observations.

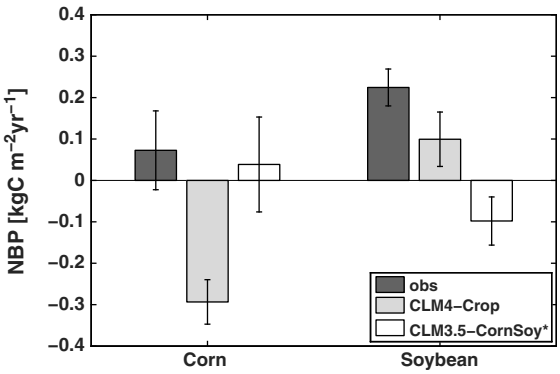

Figure 6. Evaluation of the simulated annual NBP budgets for corn and soybean. The error bars represent the standard errors of the annual NBP. The NBP of CLM3.5-CornSoy is estimated using the NEE of CLM3.5-CornSoy plus the harvested carbon calculated from yield data at the sites.

Based on our NEE EC measurements, the corn field was a carbon sink (-0.49 ± 0.12 kg C m^{-2} yr^{-1}). The uncertainty presented here was calculated as the standard error of the annual NEE. After adding the harvested grain carbon of 0.60 ± 0.09 kg C m^{-2} yr^{-1} to the annual NEE, the corn fields became a small carbon source, releasing approximately 0.07 ± 0.10 kg C m^{-2} yr^{-1} into the atmosphere (Figure 6). The CLM4-Crop-estimated annual NBP was -0.39 ± 0.05 kg C m^{-2} yr^{-1}, representing a carbon sink, mainly caused by the high bias in GPP during the early growing season. CLM3.5-CornSoy currently does not simulate the reproductive pool. The NEE in CLM3.5-CornSoy of -0.57 ± 0.05 kg C m^{-2} yr^{-1} was in close agreement with NEE measured by eddy covariance. When we added the measured yield carbon to CLM3.5-CornSoy results, the estimated NBP was 0.04 ± 0.11 kg C m^{-2} yr^{-1} and in excellent agreement with the observed values.

Soybean was almost carbon neutral with an averaged NEE of 0.02 ± 0.02 kg C m^{-2} yr^{-1} carbon released into the atmosphere based on the EC measurement. After we added the harvested carbon of 0.21 ± 0.02 kg C m^{-2} yr^{-1} into the annual carbon budget, the soybean fields became a carbon source of 0.22 ± 0.04 kg C m^{-2} yr^{-1} (Figure 6). CLM4-Crop-estimated annual soybean NBP was 0.10 ± 0.07 kg C m^{-2} yr^{-1}. However, based on the previous analyses, we know that photosynthesis was biased high in the model, but the unrealistic water stress offsets this bias. CLM3.5-CornSoy, without considering harvested carbon, gave a more negative NEE of -0.31 ± 0.04 kg C m^{-2} yr^{-1}. After we added the observed harvested carbon to the CLM3.5-CornSoy budget, it brings the annual NBP to -0.10 ± 0.06 kg C m^{-2} yr^{-1}. This value is more negative than the observed value, due to the overestimated GPP during early and late growing season (Figure 5b).

If we assume that corn and soybean are equally distributed (each take up 50% of the total 6×10^7 ha cultivated area) in the Corn Belt, and assume that the productivities observed at these two fields are typical for the Corn Belt, then the total annual NEE in the Corn Belt area would be -141 ± 99 Tg C yr^{-1}, without considering carbon removed through harvest. In an atmospheric inversion study using eight tall towers (100 m CO_2 measurement level) over the Corn Belt region (1×10^8 ha), the NEE was derived to be -178 ± 35 Tg C yr^{-1} from June to December 2007 [*Lauvaux et al.*, 2011]. These studies took a flux measurement point of view and did not consider the decomposition of the harvested grain (CO_2 leakage) outside of the flux tower footprint. If we add the harvested carbon and calculate the annual NBP, the Corn Belt becomes a carbon source of 89 ± 41 Tg C yr^{-1}. The CLM4-Crop-estimated value was -87 ± 36 Tg C yr^{-1}. This negative offset is largely due to the bias of early growing season phenology simulated in CLM4-Crop. CLM3.5-CornSoy also estimated a carbon sink with an annual NBP of -18 ± 94 Tg C yr^{-1}, presumably because of the overestimation of soybean GPP during the early and late growing season.

4. Conclusion

This study evaluated two models: CLM3.5-CornSoy and CLM4-Crop at two different corn-soybean AmeriFlux sites from 2007 to 2010. Our analyses indicate that

1. The two models with their prognostic crop phenology captured the seasonal pattern of LAI reasonably well. CLM4-Crop overestimated LAI during the early growing season, due to earlier estimation of leaf emergence, and a V_{cmax25} value that does not have seasonal variation. Both models showed positive LAI bias for both corn and soybeans for all of the growing seasons. The LAI bias of CLM3.5-CornSoy was 1.6 for corn and 2.5 for soybean. CLM4-Crop gave an LAI bias of 1.4 for corn and 2.7 for soybean. These LAI biases propagated into the energy and carbon flux simulations. Future work is needed to improve the crop phenology simulation, especially during the early growing season. For example, a V_{cmax25} with seasonal

variation should help to reduce the early growing season growth rate and thus assimilate less carbon during this period. Future studies should focus on the driving mechanisms of seasonal variations of crop photosynthesis and carbon allocation associated with leaf growth and should work to eliminate the need for setting a maximum LAI constraint.

2. Net radiation was biased high in both models and was especially pronounced for soybeans. This bias was partially compensated by using a leaf angle distribution value that was too vertical compared to field observations. The bias is likely to be more pronounced if the leaf angle distribution parameter is modified toward a more realistic value (0.17–0.12 and 0.17–0.18) as observed for corn and soybean, respectively. Here we propose that the bias in LAI (phenology) is the main cause of the net radiation bias, because higher LAI leads to a lower surface temperature and thus a positive net long-wave radiation bias. This bias has important implications for radiation balance, energy partitioning, and carbon cycling.
3. CLM4-Crop showed higher *H* and lower *LE* than observations from July to September, which we attribute to the underestimated SWC of all soil layers during this period. CLM3-Crop performed similar to CLM4-Crop to the depth of −50 cm but predicted a much wetter soil at a depth of −100 cm. This overestimated deeper soil SWC in CLM3.5-CornSoy partly offset the dry bias in the upper soil layers. Future work should focus on the mechanism of soil water dynamics especially for the deeper soil layers (lower than −15 cm).
4. Field observations indicated that both corn and soybean systems were carbon sources. However, both models underestimated the carbon emissions. Corn in CLM4-Crop and soybean in CLM3.5-CornSoy are even predicted as carbon sinks. These biases emphasize the need to improve the crop phenology simulation in Earth system models.

Acknowledgments
We express our sincere thanks to Jeremy Smith and Bill Breiter for their technical assistance in the laboratory and at the field site. Funding for this research has been provided by the National Science Foundation (ATM-0546476) and the United States Department of Agriculture (USDA-NIFA 2013-67019-21364). Funding for this AmeriFlux core site was provided by the U.S. Department of Energy's Office of Science. We are grateful to the University of Minnesota Supercomputing Institute for partial support of this work. We would like to thank Sam Levis at the National Center for Atmospheric Research for his helpful discussions and support regarding the CLM4-Crop model. We would also like to thank Mark Lostetter and Patricia Backes at the Rosemount Research and Outreach Center who provided us the yield data at the two sites. All of the meteorological and flux data used in this study are freely available at the biometeorology group UMN website (http://www.biometeorology.umn.edu/data_archive.php).

References

Allmaras, R. R., W. W. Nelson, and W. B. Voorhees (1973), Soybean and corn rooting in southwestern Minnesota: II. Root distributions, *Soil Sci. Soc. Am. J.*, *39*, 771–777.

Asner, G., and C. Wessman (1998), Variability in leaf and litter optical properties: Implications for BRDF model inversions using AVHRR, MODIS, and MISR, *Remote Sens.*, *257*, 243–257.

Baker, J. M., and T. J. Griffis (2005), Examining strategies to improve the carbon balance of corn/soybean agriculture using eddy covariance and mass balance techniques, *Agric. For. Meteorol.*, *128*(3–4), 163–177, doi:10.1016/j.agrformet.2004.11.005.

Baker, J. M., and T. J. Griffis (2008), How to build an inexpensive diffuse PAR sensor, in *28th Conference on Agricultural and Forest Meteorology*, *Am. Meteorol. Soc.*, *April 28-May 2*, *2008*, Orlando, Fla.

Baker, J. M., and T. J. Griffis (2012), A device for continuous, in situ measurement of leaf area index, in *Soil Science Society of America Meeting*, *October 21–24*, *2012*, Cincinnati, Ohio.

Barr, A. G., T. A. Black, E. H. Hogg, N. Kljun, K. Morgenstern, and Z. Nesic (2004), Interannual variability in the leaf area index of a boreal aspen-hazelnut forest in relation to net ecosystem production, *Agric. For. Meteorol.*, *126*(3–4), 237–255, doi:10.1016/j.agrformet.2004.06.011.

Betts, R. A. (2005), Integrated approaches to climate-crop modeling: Needs and challenges, *Philos. Trans. R. Soc. London, Ser. B*, *360*(1463), 2049–2065, doi:10.1098/rstb.2005.1739.

Bonan, G., and K. Oleson (2002), The land surface climatology of the Community Land Model coupled to the NCAR Community Climate Model*, *J. Clim.*, *94*, 3123–3150.

Blanken, P. D., T. A. Black, P. C. Yang, H. H. Neumann, Z. Nesic, R. Staebler, G. den Hartog, M. D. Novak, and X. Lee (1997), Energy balance and canopy conductance of a boreal aspen forest: Partitioning overstory and understory components, *J. Geophys. Res.*, *102*(D24), 28,915–28,927, doi:10.1029/97JD00193.

Bonan, G., K. Oleson, R. Fisher, G. Lasslop, and M. Reichstein (2012), Reconciling leaf physiological traits and canopy flux data: Use of the TRY and FLUXNET databases in the Community Land Model version 4, *J. Geophys. Res.*, *117*, G02026, doi:10.1029/2011JG001913.

Dai, Y., et al. (2003), The Common Land Model, *Bull. Am. Meteorol. Soc.*, *84*(8), 1013–1023, doi:10.1175/BAMS-84-8-1013.

Decker, M., and X. Zeng (2009), Impact of modified Richards equation on global soil moisture simulation in the Community Land Model (CLM3.5), *J. Adv. Model. Earth Syst.*, *1*, 1–22, doi:10.3894/JAMES.2009.1.5.

Dickinson, R., and K. Oleson (2006), The Community Land Model and its climate statistics as a component of the Community Climate System Model, *J. Clim.*, *19*, 2302–2324.

Dorman, J., and P. Sellers (1989), A global climatology of albedo, roughness length, and stomatal resistance for atmospheric general circulation models as represented by the Simple Biosphere Model, *J. Appl. Meteorol.*, *28*, 833–855.

Drewniak, B., J. Song, J. Prell, V. R. Kotamarthi, and R. Jacob (2013), Modeling agriculture in the Community Land Model, *Geosci. Model Dev.*, *6*(2), 495–515, doi:10.5194/gmd-6-495-2013.

Dwyer, L., D. Stewart, and D. Balchin (1988), Rooting characteristics of corn, soybeans, and barley as a function of available water and soil physical characteristics, *Can. J. Soil Sci.*, *68*, 121–132.

Gopalakrishnan, R., G. Bala, M. Jayaraman, L. Cao, R. Nemani, and N. H. Ravindranath (2011), Sensitivity of terrestrial water and energy budgets to CO_2 physiological forcing: An investigation using an offline land model, *Environ. Res. Lett.*, *6*(4), 1–7, doi:10.1088/1748-9326/6/4/044013.

Griffis, T. J., X. Lee, J. M. Baker, M. P. Russelle, X. Zhang, R. Venterea, and D. B. Millet (2013), Reconciling the differences between top-down and bottom-up estimates of nitrous oxide emissions for the U.S. Corn Belt, *Global Biogeochem. Cycles*, *27*, 746–754, doi:10.1002/gbc.20066.

Griffis, T., J. Baker, and J. Zhang (2005), Seasonal dynamics and partitioning of isotopic CO_2 exchange in a C_3/C_4 managed ecosystem, *Agric. For. Meteorol.*, *132*(1–2), 1–19, doi:10.1016/j.agrformet.2005.06.005.

Groisman, P., and D. Legates (1994), The accuracy of United States precipitation data, *Bull. Am. Meteorol. Soc.*, *75*(3), 215–227.

Jin, J., and N. L. Miller (2010), Regional simulations to quantify land use change and irrigation impacts on hydroclimate in the California Central Valley, *Theor. Appl. Climatol.*, *104*(3–4), 429–442, doi:10.1007/s00704-010-0352-1.

Karl, T., J. Melillo, and T. Peterson (2009), *Global Climate Change Impacts in the United States*, Cambridge Univ. Press, New York.

Kattge, J., W. Knorr, T. Raddatz, and C. Wirth (2009), Quantifying photosynthetic capacity and its relationship to leaf nitrogen content for global scale terrestrial biosphere models, *Glob. Chang. Biol.*, *15*(4), 976–991, doi:10.1111/j.1365-2486.2008.01744.x.

Keller, J., and R. D. Bliesner (1990), *Sprinkle and Trickle Irrigation*, Van Nostrand Reinhold, New York.

Kucharik, C. J. (2003), Evaluation of a process-based agroecosystem model (Agro-IBIS) across the U.S. Corn Belt: Simulations of the interannual variability in maize yield, *Earth Interact.*, *7*(14), 1–33, doi:10.1175/1087-3562(2003)007<0001:EOAPAM>2.0.CO;2.

Kucharik, C. J., et al. (2000), Testing the performance of a dynamic global ecosystem model: Water balance, carbon balance, and vegetation structure, *Global Biogeochem. Cycles*, *14*(3), 795–825, doi:10.1029/1999GB001138.

Kucharik, C., and T. Twine (2007), Residue, respiration, and residuals: Evaluation of a dynamic agroecosystem model using eddy flux measurements and biometric data, *Agric. For. Meteorol.*, *146*(3–4), 134–158, doi:10.1016/j.agrformet.2007.05.011.

Kumar, S., and V. Merwade (2011), Evaluation of NARR and CLM3.5 outputs for surface water and energy budgets in the Mississippi River basin, *J. Geophys. Res.*, *116*, D08115, doi:10.1029/2010JD014909.

Laboski, C., R. Dowdy, R. Allmaras, and J. Lamb (1998), Soil strength and water content influences on corn root distribution in a sandy soil, *Plant Soil*, *203*, 239–247.

Lauvaux, T., et al. (2011), Constraining the CO_2 budget of the Corn Belt: Exploring uncertainties from the assumptions in a mesoscale inverse system, *Atmos. Chem. Phys. Discuss.*, *11*(7), 20,855–20,898, doi:10.5194/acpd-11-20855-2011.

Lawrence, D. M., and A. G. Slater (2007), Incorporating organic soil into a global climate model, *Clim. Dyn.*, *30*(2–3), 145–160, doi:10.1007/s00382-007-0278-1.

Lawrence, D. M., et al. (2011), Parameterization improvements and functional and structural advances in version 4 of the Community Land Model, *J. Adv. Model. Earth Syst.*, *3*(3), 1–27, doi:10.1029/2011MS000045.

Lawrence, D. M., K. W. Oleson, M. G. Flanner, C. G. Fletcher, P. J. Lawrence, S. Levis, S. C. Swenson, and G. B. Bonan (2012), The CCSM4 land simulation, 1850–2005: Assessment of surface climate and new capabilities, *J. Clim.*, *25*(7), 2240–2260, doi:10.1175/JCLI-D-11-00103.1.

Lawrence, P. J., and T. N. Chase (2009), Climate impacts of making evapotranspiration in the Community Land Model (CLM3) consistent with the Simple Biosphere Model (SiB), *J. Hydrometeorol.*, *10*(2), 374–394, doi:10.1175/2008JHM987.1.

Lawrence, P. J., and T. N. Chase (2010), Investigating the climate impacts of global land cover change in the Community Climate System Model, *Int. J. Climatol.*, *30*(13), 2066–2087, doi:10.1002/joc.2061.

Levis, S. (2010), Modeling vegetation and land use in models of the Earth system, *Adv. Rev.*, *1*, 840–856.

Levis, S., G. B. Bonan, E. Kluzek, P. E. Thornton, A. Jones, W. J. Sacks, and C. J. Kucharik (2012), Interactive crop management in the Community Earth System Model (CESM1): Seasonal influences on land-atmosphere fluxes, *J. Clim.*, *25*(14), 4839–4859, doi:10.1175/JCLI-D-11-00446.1.

Li, M., and M. Zhuguo (2010), Comparisons of simulations of soil moisture variations in the Yellow River basin driven by various atmospheric forcing data sets, *Adv. Atmos. Sci.*, *2*, 1–40, doi:10.1007/s00376-010-9155-7.1.

Lobell, D. B., W. Schlenker, and J. Costa-Roberts (2011), Climate trends and global crop production since 1980, *Science*, *333*(6042), 616–20, doi:10.1126/science.1204531.

Lokupitiya, E., S. Denning, K. Paustian, I. Baker, K. Schaefer, S. Verma, T. Meyers, C. J. Bernacchi, A. Suyker, and M. Fischer (2009), Incorporation of crop phenology in Simple Biosphere Model (SiBcrop) to improve land-atmosphere carbon exchanges from croplands, *Biogeosciences*, *6*(6), 969–986, doi:10.5194/bg-6-969-2009.

Ma, S., G. Churkina, and K. Trusilova (2012), Investigating the impact of climate change on crop phenological events in Europe with a phenology model, *Int. J. Biometeorol.*, *56*(4), 749–63, doi:10.1007/s00484-011-0478-6.

Makino, A., H. Sakuma, E. Sudo, and T. Mae (2003), Differences between maize and rice in N-use efficiency for photosynthesis and protein allocation, *Plant Cell Physiol.*, *44*(9), 952–956.

Oleson, K. W., G. B. Bonan, S. Levis, and M. Vertenstein (2004a), Effects of land use change on North American climate: Impact of surface data sets and model biogeophysics, *Clim. Dyn.*, *23*(2), 117–132, doi:10.1007/s00382-004-0426-9.

Oleson, K. W., et al. (2004b), Technical description of the Community Land Model (CLM), National Center for Atmospheric Research, Boulder, Colo.

Oleson, K. W., et al. (2007), *CLM3.5 Documentation*, *Tech. Rep.*, Natl. Cent. for Atmos. Res., Boulder, Colo. [Available at http://www.cgd.ucar.edu/tss/clm/distribution/clm3.5/.]

Oleson, K. W., et al. (2008), Improvements to the Community Land Model and their impact on the hydrological cycle, *J. Geophys. Res.*, *113*, G01021, doi:10.1029/2007JG000563.

Oleson, K. W., et al. (2010), Technical description of version 4.0 of the Community Land Model (CLM), National Center for Atmospheric Research, Boulder, Colo.

Oleson, K. W., et al. (2013), Technical description of version 4.5 of the Community Land Model (CLM), National Center for Atmospheric Research, Boulder, Colo.

Piao, S., et al. (2010), The impacts of climate change on water resources and agriculture in China, *Nature*, *467*(7311), 43–51, doi:10.1038/nature09364.

Raddatz, R. L., and J. D. Cummine (2003), Interannual variability of moisture flux form the prairie agroecosystem: Impact of crop phenology on the seasonal pattern of tornado days, *Boundary Layer Meteorol.*, *106*, 283–295.

Richardson, A. D., et al. (2012), Terrestrial biosphere models need better representation of vegetation phenology: Results from the North American Carbon Program site synthesis, *Global Change Biol.*, *18*(2), 566–584, doi:10.1111/j.1365-2486.2011.02562.x.

Rosenzweig, C., et al. (2013), Assessing agricultural risks of climate change in the 21st century in a global gridded crop model intercomparison, *Proc. Natl. Acad. Sci. U.S.A.*, *14*, 1–6, doi:10.1073/pnas.1222463110.

Ross, J. (1975), Radiative transfer in plant communities, in *Vegetation and the Atmosphere*, vol. 1, edited by J. L. Monteith, pp. 13–55, Academic Press, Calif.

Ross, J., and V. Ross (1969), *Produktunost' fotosinteza v zavisimost' ot gustoty rastenii, photosynthetic Productivity of Plant Stand*, pp. 44–59, IPA, Tartu, Estonia.

Rowan, F. S., W. P. Robert, and R. S. Jeffrey (1987), The nitrogen use efficiency of C_3 and C_4 plants: II. Leaf nitrogen effects on the gas exchange characteristics of chenopodium albun (L.) and amaranthus retroflexus (L.), *Plant Physiol.*, *84*, 959–963.

Sacks, W. J., B. I. Cook, N. Buenning, S. Levis, and J. H. Helkowski (2008), Effects of global irrigation on the near-surface climate, *Clim. Dyn.*, *33*(2–3), 159–175, doi:10.1007/s00382-008-0445-z.

Sakaguchi, K., and X. Zeng (2009), Effects of soil wetness, plant litter, and under-canopy atmospheric stability on ground evaporation in the Community Land Model (CLM3.5), *J. Geophys. Res.*, *114*, D01107, doi:10.1029/2008JD010834.

Sakaguchi, K., X. Zeng, B. J. Christoffersen, N. Restrepo-Coupe, S. R. Saleska, and P. M. Brando (2011), Natural and drought scenarios in an east central Amazon forest: Fidelity of the Community Land Model 3.5 with three biogeochemical models, *J. Geophys. Res.*, *116*, G01029, doi:10.1029/2010JG001477.

Schaefer, K., et al. (2012), A model-data comparison of gross primary productivity: Results from the North American Carbon Program site synthesis, *J. Geophys. Res.*, *117*, G03010, doi:10.1029/2012JG001960.

Schepers, J., T. Blackmer, W. Wilhelm, and M. Resende (1996), Transmittance and reflectance measurements of corn leaves from plants with different nitrogen and water supply, *J. Plant Physiol.*, *148*, 523–529.

Schmitt, M. R., and G. E. Edwards (1981), Photosynthetic capacity and nitrogen use efficiency of maize, wheat, and rice: A comparison between C_3 and C_4 photosynthesis, *J. Exp. Bot.*, *32*(3), 459–466.

Sheffield, J., G. Goteti, and E. F. Wood (2006), Development of a 50 year high-resolution global data set of meteorological forcings for land surface modeling, *J. Clim.*, *19*(13), 3088–3111, doi:10.1175/JCLI3790.1.

Stöckli, R., D. M. Lawrence, G.-Y. Niu, K. W. Oleson, P. E. Thornton, Z.-L. Yang, G. B. Bonan, A. S. Denning, and S. W. Running (2008), Use of FLUXNET in the Community Land Model development, *J. Geophys. Res.*, *113*, G01025, doi:10.1029/2007JG000562.

Thornton, P. E., and N. A. Rosenbloom (2005), Ecosystem model spin-up: Estimating steady state conditions in a coupled terrestrial carbon and nitrogen cycle model, *Ecol. Modell.*, *189*(1–2), 25–48, doi:10.1016/j.ecolmodel.2005.04.008.

Thornton, P. E., J.-F. Lamarque, N. A. Rosenbloom, and N. M. Mahowald (2007), Influence of carbon-nitrogen cycle coupling on land model response to CO_2 fertilization and climate variability, *Global Biogeochem. Cycles*, *21*, GB4018, doi:10.1029/2006GB002868.

Thornton, P. E., S. C. Doney, K. Lindsay, J. K. Moore, N. Mahowald, J. T. Randerson, I. Fung, J.-F. Lamarque, J. J. Feddema, and Y.-H. Lee (2009), Carbon-nitrogen interactions regulate climate-carbon cycle feedback: Results from an atmosphere-ocean general circulation model, *Biogeosciences*, *6*(10), 2099–2120, doi:10.5194/bg-6-2099-2009.

Twine, T. E., and C. J. Kucharik (2009), Climate impacts on net primary productivity trends in natural and managed ecosystems of the central and eastern United States, *Agric. For. Meteorol.*, *149*(12), 2143–2161, doi:10.1016/j.agrformet.2009.05.012.

Upton, G. J. G., and A. R. Rahimi (2003), On-line detection of errors in tipping-bucket rain gauges, *J. Hydrol.*, *278*(1–4), 197–212, doi:10.1016/S0022-1694(03)00142-2.

Walter-Shea, E., and J. Norman (1991), Leaf reflectance and transmittance in soybean and corn, *Agron. J.*, *83*, 631–636.

Walter-Shea, E., J. Norman, and B. Blad (1989), Leaf bidirectional reflectance and transmittance in corn and soybean, *Remote Sens. Environ.*, *29*, 161–174.

Wang, A., and X. Zeng (2011), Sensitivities of terrestrial water cycle simulations to the variations of precipitation and air temperature in China, *J. Geophys. Res.*, *116*, D02107, doi:10.1029/2010JD014659.

Wilson, K., et al. (2002), Energy balance closure at FLUXNET sites, *Agric. For. Meteorol.*, *113*(1–4), 223–243, doi:10.1016/S0168-1923(02)00109-0.

Wullschleger, S. (1993), Biochemical limitations to carbon assimilation in C3 plants: A retrospective analysis of the A/Ci curves from 109 species, *J. Exp. Bot.*, *44*(262), 907–920.

Xiao, W., X. Lee, T. J. Griffis, K. Kim, L. R. Welp, and Q. Yu (2010), A modeling investigation of canopy-air oxygen isotopic exchange of water vapor and carbon dioxide in a soybean field, *J. Geophys. Res.*, *115*, G01004, doi:10.1029/2009JG001163.

Yin, X. (2013), Improving ecophysiological simulation models to predict the impact of elevated atmospheric CO_2 concentration on crop productivity, *Ann. Bot.*, *112*(3), 465–475, doi:10.1093/aob/mct016.

Yuan, X., and X.-Z. Liang (2011), Evaluation of a Conjunctive Surface–Subsurface Process Model (CSSP) over the contiguous United States at regional-local scales, *J. Hydrometeorol.*, *12*(4), 579–599, doi:10.1175/2010JHM1302.1.

Zeng, X., and M. Decker (2009), Improving the numerical solution of soil moisturebbased Richards equation for land models with a deep or shallow water table, *J. Hydrometeorol.*, *10*(1), 308–319, doi:10.1175/2008JHM1011.1.

Zeng, X., M. Shaikh, and Y. Dai (2002), Coupling of the common land model to the NCAR Community Climate Model, *J. Clim.*, *15*, 1832–1854.